



## Original Articles

# Carbohydrate-based adjuvants activate tumor-specific Th1 and CD8<sup>+</sup> T-cell responses and reduce the immunosuppressive activity of MDSCs

Xiaojing Xu<sup>a</sup>, Ziqi Jin<sup>b</sup>, Yonghao Liu<sup>b</sup>, Huanle Gong<sup>b</sup>, Qing Sun<sup>c</sup>, Weidong Zhang<sup>d,\*</sup>,  
Lixiang Zhao<sup>e,\*\*</sup>

<sup>a</sup> Department of Cell Biology, College of Basic Medicine and Biological Sciences, Medical Department, Soochow University, 215123, Suzhou, PR China

<sup>b</sup> Institute of Blood and Marrow Transplantation, Department of Hematology, Collaborative Innovation Center of Hematology, The First Affiliated Hospital of Soochow University, Suzhou, PR China

<sup>c</sup> Virus Research Unit, Department of Microbiology and Immunology, School of Medicine, University of Otago, Dunedin, New Zealand

<sup>d</sup> Center for Soft Condensed Matter Physics and Interdisciplinary Research & School of Physical Science and Technology, Soochow University, Suzhou, 215006, PR China

<sup>e</sup> Department of Immunology, College of Basic Medicine and Biological Sciences, Medical Department, Soochow University, 215123, Suzhou, PR China



## A B S T R A C T

Toll-like receptors (TLRs) and C-type lectin receptors (CLRs) contribute to antigen capture, uptake, presentation and activation of immune responses. We recently developed a new and lymph node (LN) targeting adjuvant (D-CpG) by chemical conjugation type B CpG DNA with FDA-approved dextran polymer for lymph node imaging. To elucidate the possible antitumor mechanisms of this adjuvant, prophylaxis and therapeutic models of melanoma were used in this study. Our results showed that D-CpG was an efficient adjuvant of protein-based tumor vaccine in both prophylaxis and therapeutic models. It enhanced the tumor-specific Th1 and CTL responses. It also facilitated the tumor infiltration of the T cells and promoted IFN $\gamma$  and TNF $\alpha$  production of both CD4<sup>+</sup> and CD8<sup>+</sup> T cells. In therapeutic model, D-CpG included tumor vaccine decreased the percentage of CD11b<sup>+</sup>Gr1<sup>low</sup> MDSCs in spleen and inhibited their infiltration in tumor microenvironments. Administration of the D-CpG included vaccine significantly inhibited lung metastasis of the tumor through similar mechanisms. In conclusion, D-CpG used as tumor vaccine adjuvant can enhance both Th1 and CTL responses and inhibit CD11b<sup>+</sup>Gr1<sup>low</sup> MDSCs, which may have general applicability to the development of vaccines against tumors.

## 1. Introduction

Both type 1 helper T (Th1) and cytotoxic T lymphocytes (CTLs) were required during the eradication of tumor [1–3]. Induction of both Th1 and CTL responses is one of the most sought-after goals in cancer immunotherapy. Vaccines have been widely used in many infectious diseases. However, tumor vaccines have not succeeded in cancer immunotherapy, as the poor induction of both Th1 and TC1 responses and the immunosuppressive microenvironment [4,5].

To enhance CD4<sup>+</sup> T and CD8<sup>+</sup> T responses, adjuvants are routinely used to vaccine formulations [6,7]. However, limited vaccine adjuvants are currently approved for human use. Agonists of Toll-like receptors (TLRs) activate the innate immunity and support the subsequent development of adaptive immunity, which makes them attractive candidates of vaccine adjuvants to improve immune responses [8–10]. Among different TLRs, TLR9 senses unmethylated cytosine-phosphate-guanine (CpG) dinucleotides, which are relatively common in bacterial and viral DNA, but not in vertebrate [11–13]. Activation of TLR9 can induce the secretion of cytokines (such as IFN $\gamma$ ) and expansion of T-cell

populations, particularly Th1 cells and CTLs [14–18]. Therefore, agonists of TLR9 (CpG) have a potential to stimulate both Th1 and CTLs, which makes it a candidate of adjuvants of tumor vaccines [19,20]. Although clinical trials indicated that CpG enhanced the development of antitumor T-cell responses when used as tumor vaccine adjuvants, strategies for improving the therapeutic potential of CpG used as tumor vaccine adjuvants are warranted. Previously, we developed a new adjuvant (D-CpG) by chemical conjugation of type B CpG DNA to dextran employed as the LN targeting carrier, which exhibited a long-lasting therapeutic effect than unconjugated CpG in mice tumor model [21]. However, the mechanisms underlying the antitumor activity of D-CpG used as protein-based tumor vaccine are not clear.

In the current study, we used prophylaxis and therapeutic models to elucidate the effects and possible mechanisms of D-CpG included tumor vaccine *in vivo*. Our results showed that D-CpG was an efficient adjuvant of protein-based tumor vaccine in both prophylaxis and therapeutic models. It enhanced the tumor-specific Th1 and CTL responses and inhibited CD11b<sup>+</sup>Gr1<sup>low</sup> MDSCs, which may have general applicability to the development of vaccines against tumors.

\* Corresponding author.

\*\* Corresponding author.

E-mail addresses: [zhangweidong@suda.edu.cn](mailto:zhangweidong@suda.edu.cn) (W. Zhang), [zhaolixiang@suda.edu.cn](mailto:zhaolixiang@suda.edu.cn) (L. Zhao).

## 2. Materials and methods

### 2.1. Animals

Specific-pathogen-free (SPF) 6-week-old female C57BL/6 mice were purchased from the Shanghai Laboratory Animal Center (Shanghai, China). OT-I mice were provided by Prof. Zhinan Yin (Nankai University, Tianjin, PR China). Mouse care and experimental procedures were performed under SPF conditions. All animal protocols were approved by the ethics committee of Soochow University, and all *in vivo* experiments were performed according to the National Institutes of Health Guide for the Care and Use of Laboratory Animals. At the end of the experiments, animals were euthanized in a CO<sub>2</sub>-containing chamber.

### 2.2. Cell lines

B16-OVA and B16-F10 cells obtained from the American Type Culture Collection in 2011 were cultured in complete DMEM medium (Gibco) with 10% FBS. Tumor cells were passaged when they reached 80%–90% confluence, and cells used in this study were not passaged more than three times. Cells were cytogenetically tested with negative were performed with negative results before use.

### 2.3. Animal models

In prophylactic models, mice were immunized s.c. at the left flank with one of three vaccines (PBS and 10 µg OVA (PBS + OVA), 10 µg OVA and 1.24 nmol CpG (CpG + OVA), or 10 µg OVA and 1.24 nmol D-CpG (D-CpG + OVA)) in a total volume of 100 µL, and the injections were repeated 1-wk later. Two weeks after last immunization,  $1.5 \times 10^5$  B16-OVA cells were s.c. implanted into the right flank of mice. Tumor volumes were monitored and calculated using formula  $V = (L \times W^2)/2$ , where L is the length (longest dimension), and W is the width (shortest dimension).

In therapeutic experiments on subcutaneous model, mice were s.c. inoculated at the right flank with  $1.5 \times 10^5$  B16-OVA cells, and immunized s.c. with tumor vaccines at the left flank 8 and 13 days post tumor inoculation, respectively. The tumor sizes were daily measured from day 5 post tumor inoculation.

In metastasis model, mice were injected i.v. with  $4 \times 10^5$  B16-OVA from tail vein. Tumor vaccines were injected s.c. at the left flank 8 and 13 days post tumor inoculation. 7 days later, mice were sacrificed and lungs were removed, and the metastatic nodules were counted.

As for survival experiments, tumor-bearing mice were observed up to 40 days in preventive model and 45 days in therapeutic models post tumor injection.

### 2.4. Cell preparation from spleens and tumors

The spleen was gently homogenized, and splenocytes were collected by filtering through a 70-mm nylon mesh. TILs were prepared by processing the tissues into single-cell suspensions, and lymphocytes were separated on a 40% Percoll (GE Healthcare) gradient. Red blood cells were lysed.

### 2.5. *In vitro* T-cell proliferation and MDSCs inhibition assay

DCs isolated from spleens were loaded with OVA protein for about 24 h. In the proliferation experiment, CD4<sup>+</sup> and CD8<sup>+</sup> T cells (15,000) were co-cultured with 3000 irradiated OVA-loaded DCs in a 96-well cell culture plate (Corning Costar), respectively. In MDSC inhibition experiment, CD8<sup>+</sup> T (50,000) cells from OT-1 mice were co-cultured with CD11b<sup>+</sup>Gr1<sup>low</sup> or CD11b<sup>+</sup>Gr1<sup>high</sup> cells isolated from tumor-bearing mice at different ratios in the presence of 10,000 irradiated OVA-loaded DCs. All of co-cultured cells were maintained in RPMI 1640 medium

supplemented with 10% fetal bovine serum and 20 IU/mL recombinant IL2 (Beijing Four Rings Bio-Pharmaceutical). <sup>3</sup>H-thymidine (Shanghai Institute of Physics, Chinese Academy of Sciences, Shanghai, China) were added to the co-culture 72 h later. After another 16 h, incorporation of <sup>3</sup>H-thymidine was measured with a liquid scintillation counter (PerkinElmer Instruments). The proliferation of T cells was also examined by detection of PCNA expression with western blot.

### 2.6. Cytotoxicity assay

Splenocytes (effector) were diluted and cultured with B16-OVA (6500 cells/well, target) in a 96-well plate at effector/target ratios of 100:1, 50:1 and 25:1 at 37 °C in a 5% CO<sub>2</sub>. Cytotoxicity was measured by CytoTox 96 nonradioactive cytotoxicity assay (Promega). The percentage of lysis was calculated using the following formula: (experimental - effector spontaneous - target spontaneous) × 100/(target maximum - target spontaneous).

### 2.7. Flow cytometry

Monoclonal antibodies were purchased from BD Biosciences and Biolegend: anti-CD4-FITC (RM4-5), anti-NK1.1-FITC (PK136), anti-CD19-FITC (1D3), anti-IL2-FITC (JES6-5H4), anti-CD3e-PE (145-2C11), anti-IL4-PE (11B11), anti-IFN $\gamma$ -PE (XMG1.2), anti-CD8a-PerCP Cy5.5 (53-6.7), anti-Gr1-PE, anti-Gr1-PerCP Cy5.5 (RB6-8C5), anti-CD11b-PE-Cy7 (M1/70), anti-CD44-PE (IM7), anti-CD45-APC (30-F11) anti-CD62L-FITC (MEL-14), anti-CD11c-PE-Cy7 (HL3), anti-F4/80-FITC (BM8), anti-CD16/32-PE (93), anti-CD206-PE (C068C2), anti-PD1-APC (29F.1A12), anti-PDL1-APC(10F.9G2), anti-CTLA4-PE(9H10) and anti-TNF $\alpha$ -APC (MP6-XT22). Cells stainings were performed in FACS buffer (PBS containing 1% BSA, 0.2 mM EDTA, and 0.1% NaN<sub>3</sub>) supplemented with purified anti-CD16/32 for 30 min at 4 °C. The flow cytometric results were analyzed with FACS CantoII (BD Biosciences) using CellQuest software.

### 2.8. Tetramer staining

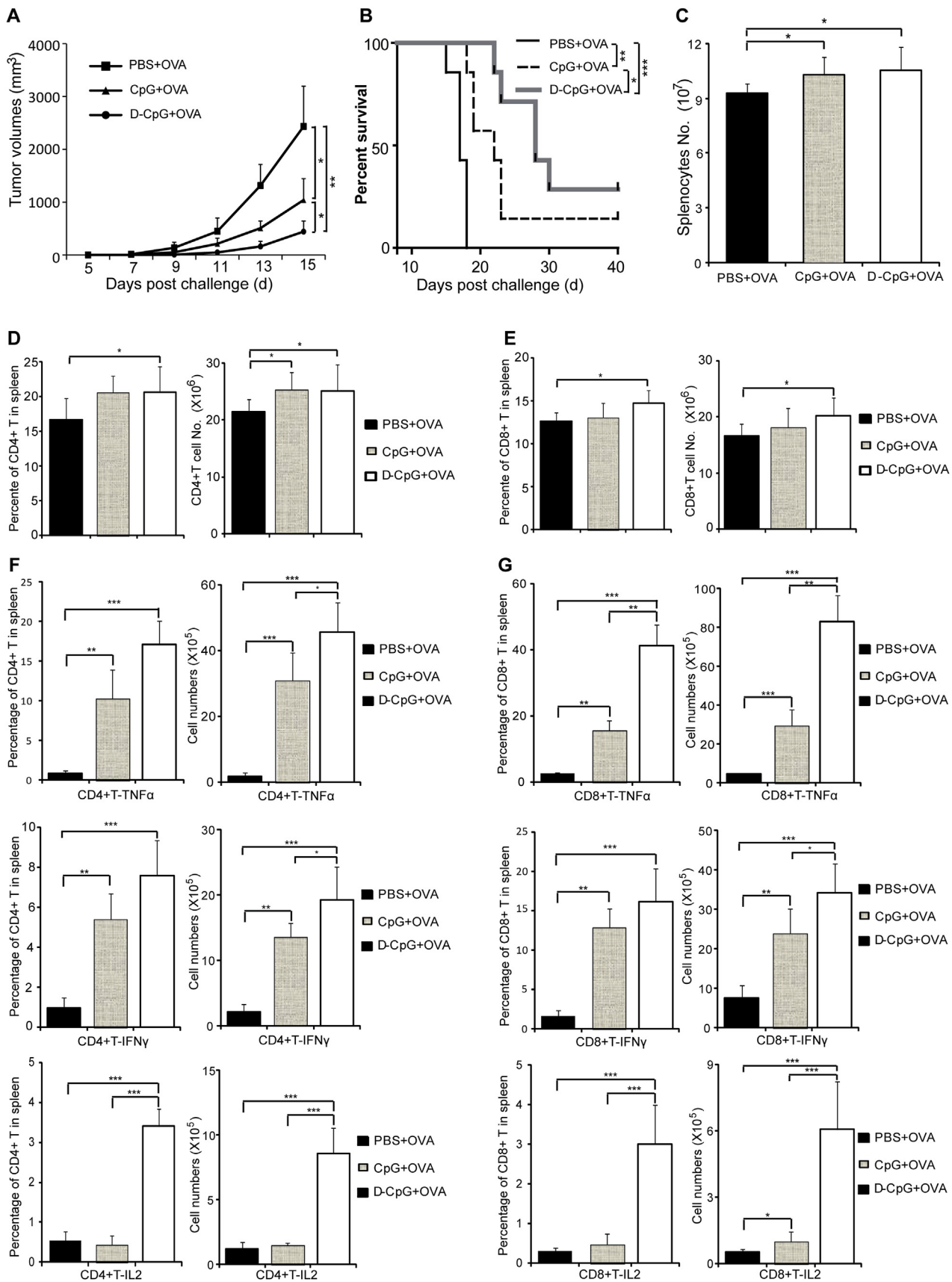
TILs were blocked with Fc-blocker and stained with PE-labeled tetramers (Beckman Coulter) and anti-CD8-APC for 30 min at room temperature. Cells were washed, resuspended in FACS buffer and analyzed with FACS CantoII (BD Biosciences).

### 2.9. *In vivo* T-cell and MDSCs depletion

For CD4<sup>+</sup> or/and CD8<sup>+</sup> T cells depletion, mice were injected i.p. with 1 mg of GK1.5 (rat anti-mouse CD4mAb, Sungene Biotech) or/and 53-6.7 (rat anti-mouse CD8 mAb, Sungene Biotech) 2 days before immunization with vaccines, and the injections were repeated 7 days later. To deplete MDSCs, 250 µg of RB6-8C5 (rat anti-mouse Gr1 Ab, Abcam) were injected i.p. on the same day of vaccination, and antibody injections were repeated 7 days later. The efficacy of cell depletion was confirmed by flow cytometric analysis.

### 2.10. Immunohistochemistry and histopathology

Paraffin sections of tissue were sequentially deparaffinized and incubated with various primary antibodies, including GK1.5 (rat anti-mouse CD4 Ab, Abcam) or 2.43 (rat anti-mouse CD8 Ab, Abcam) overnight at 4 °C, followed by incubation with HRP-conjugated rabbit anti-rat IgG (Abcam). The presence of protein of interest was visualized by DAB staining, and nuclear counter-staining was performed with hematoxylin (Solarbio). Slides were examined by a pathologist who was blinded for the experimental history of the animals.



(caption on next page)

**Fig. 1. Prophylaxis effect of D-CpG included tumor vaccine.**(A) Tumor growth curves of melanoma model. Mice were immunized with PBS + OVA, CpG + OVA, or D-CpG + OVA twice with 1-wk intervals, respectively, then the mice were injected with  $1.5 \times 10^5$  B16-OVA cells 2 wk after the last immunization. The tumor volumes were monitored daily. (B) Kaplan – Meier survival of mice were monitored over time. (C–G) Mice were sacrificed on day 10 after the last immunization, and single cell suspensions of spleen were prepared to analyze the numbers of total splenocytes (C), CD4<sup>+</sup> T cells (D) and CD8<sup>+</sup> T cells (E) by flow cytometry. The frequencies and total numbers of IFN $\gamma$ -, TNF $\alpha$ - and IL2-producing CD4<sup>+</sup> T cells (F) and CD8<sup>+</sup> T cells (G) by flow cytometry. The experiments were performed with five to seven mice per group. The assays were done in quadruplicates. The data shown are the representative of three experiments. \**p* < 0.05 and \*\**p* < 0.01, \*\*\**p* < 0.001.

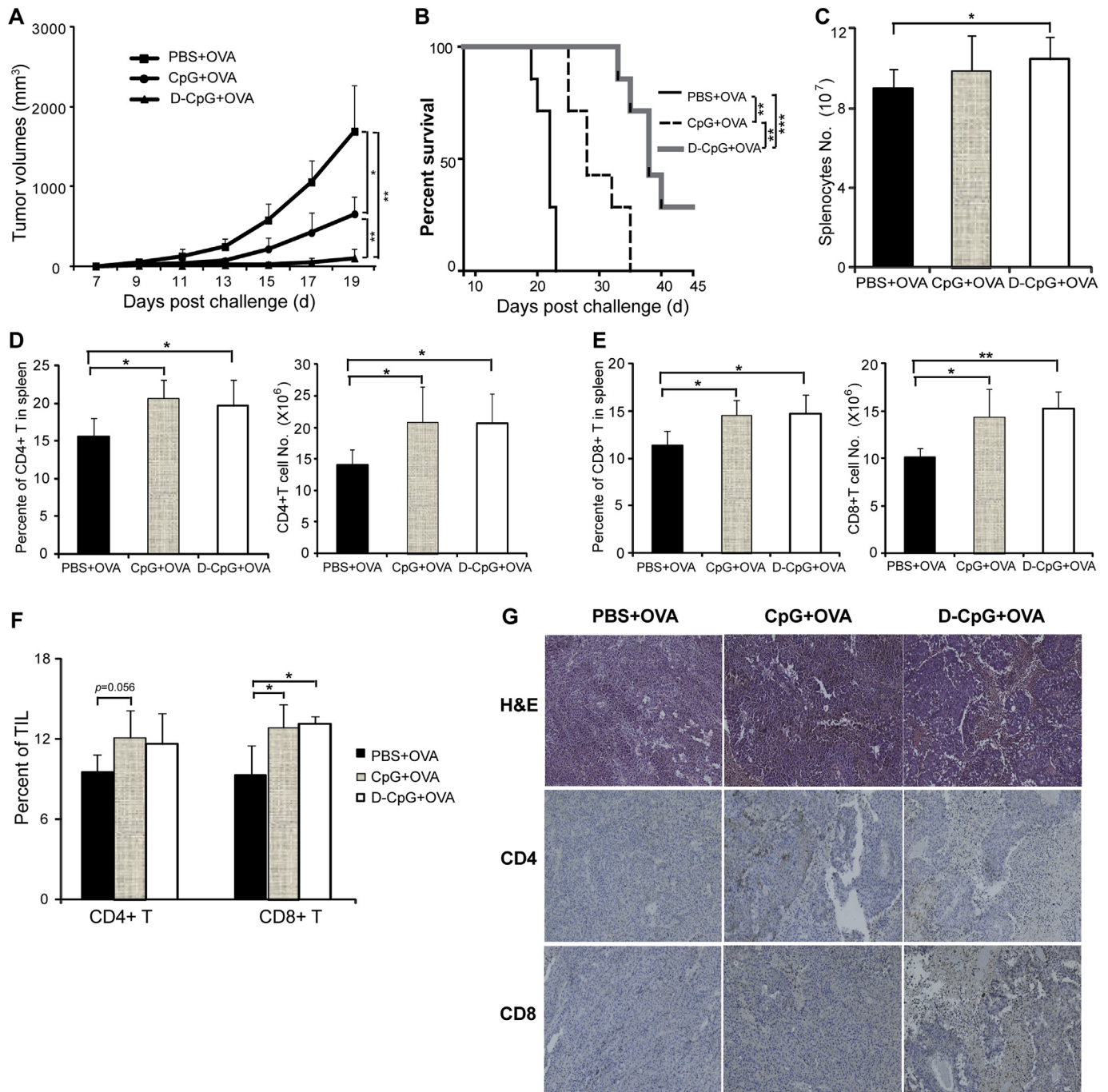
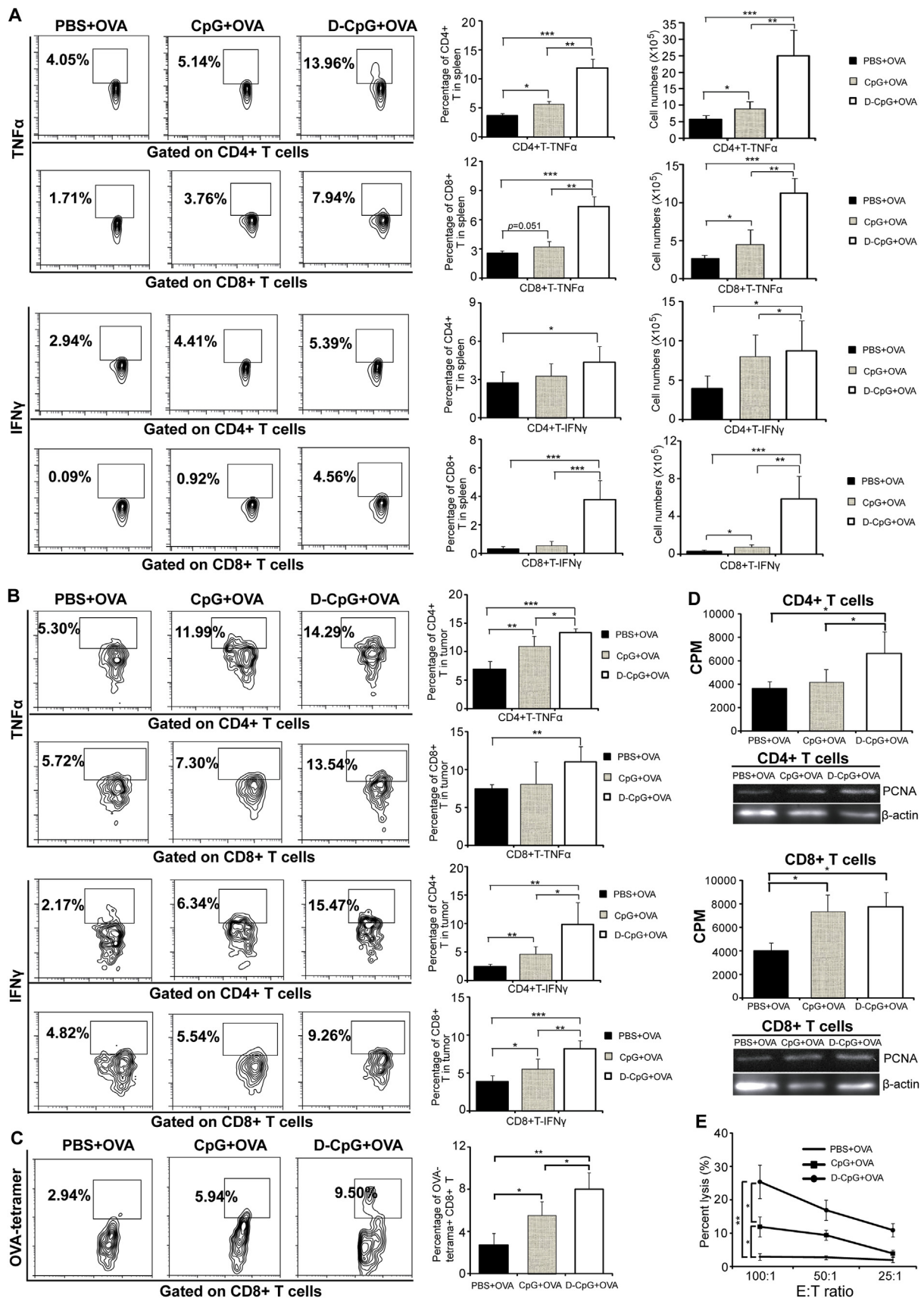


**Fig. 2. Therapeutic effects of D-CpG included tumor vaccine in subcutaneous melanoma model.**(A) Tumor growth of melanoma-bearing mice. Mice were injected with  $1.5 \times 10^5$  B16-OVA cells, and immunized s.c. with one of the three tumor vaccines at the left flank 8 and 13 days post tumor inoculation, respectively. (C–G) Mice were sacrificed on day 18 after tumor inoculation. Total cell numbers of splenocytes (C), frequencies and total cell numbers of CD4<sup>+</sup> T (D), and CD8<sup>+</sup> T (E) cells in the spleen and frequencies of tumor-infiltrating CD4<sup>+</sup> T and CD8<sup>+</sup> T cells (F) were analyzed by flow cytometry. (G) H&E and immunohistochemical staining for CD4<sup>+</sup> and CD8<sup>+</sup> T cells of tumor tissues from melanoma-bearing mice (100 × magnification). The data shown are the representative of at least three experiments. \**p* < 0.05 and \*\**p* < 0.01, \*\*\**p* < 0.001.



(caption on next page)

**Fig. 3. D-CpG included tumor vaccine promoted the production of tumor-specific Th1 cytokine from both CD4<sup>+</sup> T and CD8<sup>+</sup> T cells in a primary tumor model.** (A) Intracellular staining of TNF $\alpha$  and IFN $\gamma$  of CD4<sup>+</sup> T and CD8<sup>+</sup> T cells from splenocytes stimulated with OVA proteins. (B) Intracellular staining of TNF $\alpha$  and IFN $\gamma$  of CD4<sup>+</sup> and CD8<sup>+</sup> T cells from TILs stimulated with OVA proteins. (C) Tetramer staining of OVA-specific CD8<sup>+</sup> T cells in TILs. (D) Proliferations of CD4<sup>+</sup> T and CD8<sup>+</sup> T cells from the spleens of tumor-bearing mice stimulated with irradiated OVA-loaded DCs were measured by <sup>3</sup>H-thymidine incorporation assay and PCNA expression using western blot. (E) Cytotoxicity assay of splenocytes from the tumor-bearing mice against B16-OVA tumor cells. Splenocytes from tumor-bearing mice were incubated with OVA protein for 5 days and used as effector cells, and then co-cultured with B16-OVA at various ratios. The specific killings were determined using CytoTox 96 nonradioactive cytotoxicity assay. The experiments were performed with five to seven mice per group. The assays were done in quadruplicates. The data shown are the representative of at least three experiments. \**p* < 0.05 and \*\**p* < 0.01, \*\*\**p* < 0.001.

### 2.11. Statistical analysis

Experiments were performed at a minimum of triplicate. Data were analyzed using a one-way analysis of variance (ANOVA) with the Tukey's post-hoc test for statistical evaluation, and presented as the mean standard error of the mean (SEM). Log-Rank test was performed on the Kaplan–Meier survival curves. Data were analyzed using GraphPad Prism 5 software for Windows (GraphPad Software, San Diego, CA), and differences were considered statistically significant when *p* < 0.05. The significance levels are marked \**p* < 0.05, \*\**p* < 0.01, and \*\*\**p* < 0.001.

## 3. Results

### 3.1. Prophylactic effects of protein-based vaccine formulated with D-CpG

In prophylaxis model, mice immunized with D-CpG + OVA had significant reduction in tumor growth (Fig. 1A). The reduction of tumor growth was also correlated with an increase in survival (Fig. 1B). Splenocytes from immunized mice were analyzed by flow cytometry 10 days post last vaccination (Fig. 1C–E). Percentages and total numbers of CD4<sup>+</sup> T and CD8<sup>+</sup> T cells were significantly enhanced after D-CpG + OVA immunization. The percentages and total numbers of other immune cells were similar in each group (Fig. S1). Antigen-specific T-cell responses were examined by intracellular staining (Fig. 1F–G). D-CpG + OVA immunized mice exhibited significantly increased production of TNF $\alpha$ , IFN $\gamma$  and IL2 in CD4<sup>+</sup> T and CD8<sup>+</sup> T cells. These data suggested that D-CpG enhanced tumor-specific Th1 and Tc1 responses in prophylaxis model.

### 3.2. Therapeutic benefits of D-CpG included vaccine in a primary tumor model

In primary tumor model, tumor-bearing mice were injected s.c. with vaccines on day 8 and 13. As shown in Fig. 2A, tumor growth was effectively controlled in mice immunized with CpG + OVA compared with PBS + OVA. Notably, tumor growth was significantly inhibited in D-CpG + OVA group, as compared with CpG + OVA and PBS + OVA groups. The reduction of tumor growth was also correlated with an increase in survival (Fig. 2B).

To elucidate possible mechanisms of antitumor effects induced by D-CpG + OVA, immune cell subtypes in the spleens were analyzed by flow cytometry on day 18 after tumor inoculation. The total numbers of splenocytes were significantly higher in D-CpG + OVA group than PBS + OVA group (Fig. 2C). The percentages and absolute numbers of both CD4<sup>+</sup> T and CD8<sup>+</sup> T in spleen significantly increased in D-CpG + OVA groups (Fig. 2D–E). Percentages and total numbers of other immune cells in spleen were not significantly different among each group (Fig. S2).

Tumor-infiltrating lymphocytes (TILs) were phenotypically analyzed by flow cytometry, and significantly increased tumor infiltrations of CD8<sup>+</sup> T cells were observed in mice immunized with CpG + OVA or D-CpG + OVA compared with PBS + OVA group (Fig. 2F). These results were also confirmed by H&E staining and immunohistochemical staining (Fig. 2G). Mice treated with D-CpG + OVA exhibited significantly increased expressions of PD-1 on both CD4<sup>+</sup> and CD8<sup>+</sup> T

cells (Fig. S3A), but CTLA-4 expression on T cells were not affected (Fig. S3B). All of the tumor cells expressed PD-L1, and mice treated with D-CpG + OVA exhibited significantly increased expressions levels of PD-L1 on tumor cells (Fig. S3C). Percentages of Tregs were similar in each group (Fig. S3D).

### 3.3. CD4<sup>+</sup> and CD8<sup>+</sup> T cells activated by D-CpG included vaccine in a primary tumor model

T-cell responses from splenocytes and TILs were determined by stimulation with OVA protein using intracellular staining (Fig. 3A–B). In spleen, the percentages and numbers of TNF $\alpha$ - or IFN $\gamma$ -producing CD4<sup>+</sup> and CD8<sup>+</sup> T cells were significantly enhanced in D-CpG + OVA group. CD4<sup>+</sup> and CD8<sup>+</sup> T cells from CpG + OVA group also exhibited significantly higher TNF $\alpha$  production than PBS + OVA group. As for TILs, the percentages of TNF $\alpha$ - or IFN $\gamma$ -producing CD4<sup>+</sup> T and CD8<sup>+</sup> T cells were significantly high in D-CpG + OVA group (Fig. 3B).

The percentages of OVA-specific CD8<sup>+</sup> T cells in TILs significantly increased in D-CpG + OVA immunized mice (Fig. 3C). <sup>3</sup>H-thymidine incorporation assay showed that the proliferations of OVA-specific CD4<sup>+</sup> and CD8<sup>+</sup> T cells were significantly high in D-CpG + OVA group, which was confirmed by the PCNA expression (Fig. 3D). Splenocytes from D-CpG + OVA immunized mice exhibited the highest killing capacity against B16-OVA cells (Fig. 3E). All these results demonstrated that D-CpG + OVA promoted both tumor-specific CD4<sup>+</sup> and CD8<sup>+</sup> T-cell responses in primary tumor model.

### 3.4. Therapeutic benefits of D-CpG in melanoma lung metastasis model

To assess whether D-CpG included vaccine could protect mice from tumor metastasis, mice injected i.v. with B16-OVA were s.c. immunized with vaccines at day 8 and 13 post tumor injection. CpG + OVA or D-CpG + OVA treatment dramatically reduced the number of lung metastases compared with PBS + OVA-treated group (Fig. 4A). Moreover, immunization with D-CpG + OVA significantly reduced the number of lung metastases compared with CpG + OVA. The reduction of lung metastases was also correlated with an increase in survival (Fig. 4B).

To elucidate possible mechanisms of antitumor effects induced by D-CpG + OVA, splenocytes and TILs were analyzed by flow cytometry on day 17 after tumor inoculation. D-CpG + OVA immunization dramatically enhanced percentages and numbers of CD4<sup>+</sup> and CD8<sup>+</sup> T cells in spleen (Fig. 4C–E). Tumor-infiltrating CD4<sup>+</sup> and CD8<sup>+</sup> T cells in TILs also increased, which was confirmed by H&E staining and immunohistochemical staining (Fig. 4F–G). In spleen, prevalence and total numbers of other immune cells were similar in each group (Fig. S4A). Although the prevalence of M1 macrophages in D-CpG + OVA group increased in TILs, but the difference was not significant. Percentages of other immune cells were similar in TIL of each group (Fig. S4B). D-CpG + OVA treatment increased PD-1 and CTLA-4 expressions on tumor-infiltrating T cells, and PD-L1 expression levels on tumor cells, but the differences were not significant (Figs. S5A–C). Percentages of Tregs were similar in each group (Fig. S5D).

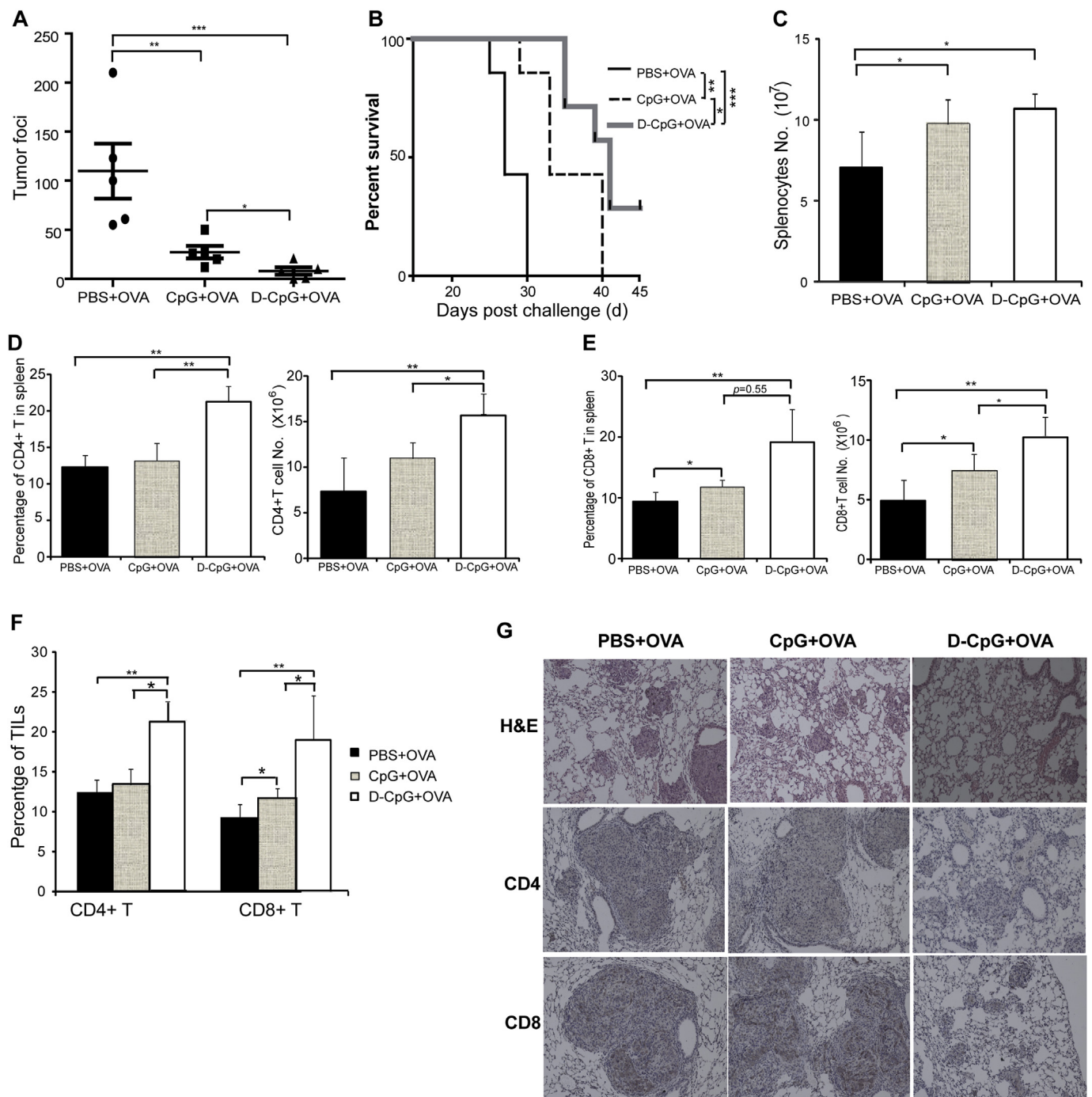


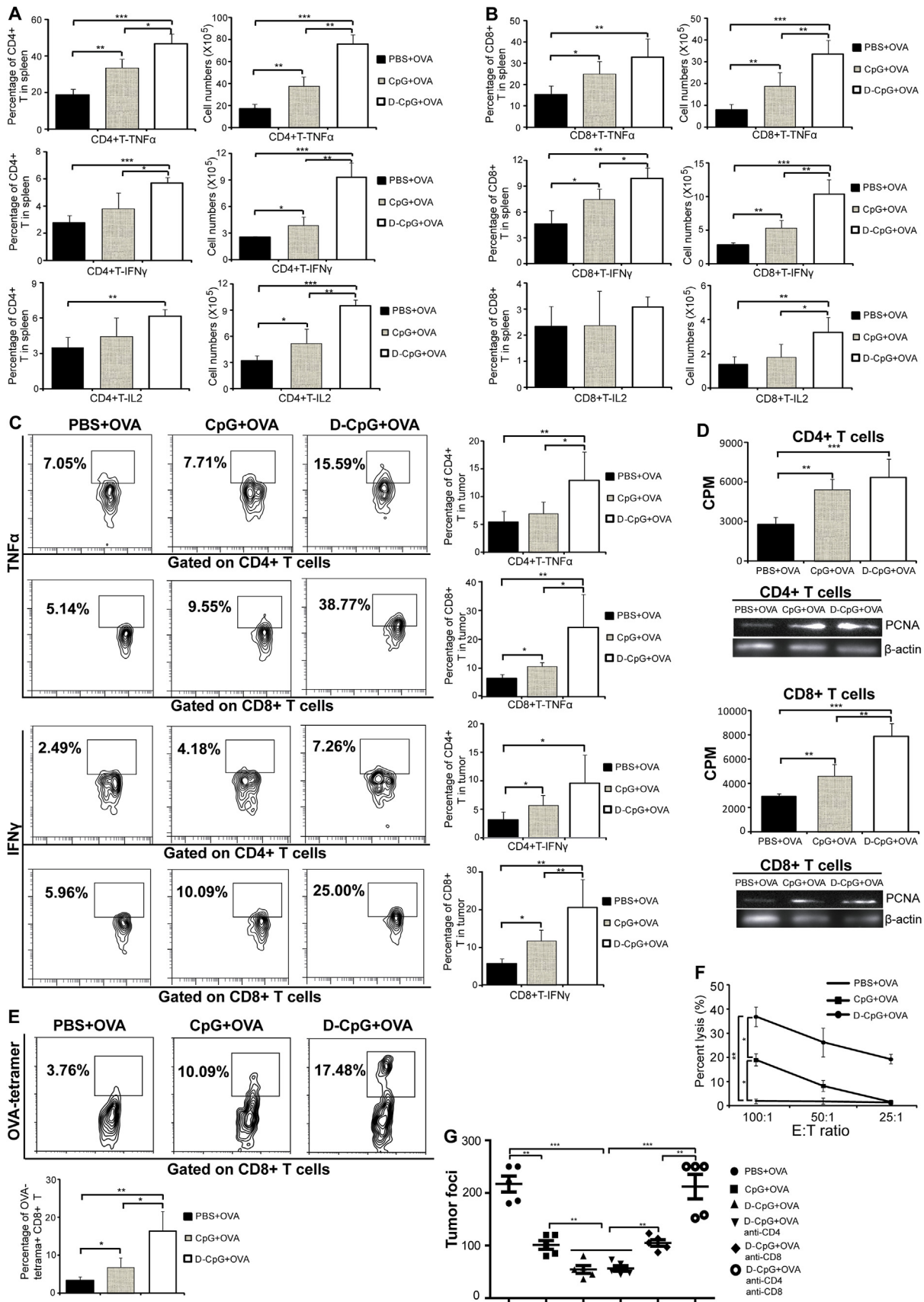
**Fig. 4. Therapeutic effects of D-CpG included tumor vaccine in lung metastasis model.**

(A) The numbers of metastatic nodules in the lungs of the tumor-bearing mice. Mice were injected i.v. with  $4 \times 10^5$  B16-OVA from tail vein. At day 8 and 13 post tumor inoculation, mice were immunized with PBS + OVA, CpG + OVA or D-CpG + OVA, respectively. (B) Kaplan – Meier survival of mice were monitored over time. (C–G) Seven days later, mice were sacrificed, and the metastatic nodules in lungs were quantified. The numbers of splenocytes (C), the percentages and total numbers of CD4<sup>+</sup> T cells (D) and CD8<sup>+</sup> T cells (E) were determined by flow cytometry. (F) The percentages of CD4<sup>+</sup> T and CD8<sup>+</sup> T cells were determined by flow cytometry. (G) H&E and immunochemical staining for CD4<sup>+</sup> and CD8<sup>+</sup> T cells of tumor tissues from melanoma-bearing mice (100 × magnification). The experiments were performed with five to seven mice per group. The assays were done in quadruplicates. The data shown are the representative of at least three experiments. \**p* < 0.05 and \*\**p* < 0.01, \*\*\**p* < 0.001.

**3.5. Antigen-specific CD4<sup>+</sup> and CD8<sup>+</sup> T cells are critical for the antitumor effects in metastasis model**

Antigen-specific T-cell responses of mice with lung metastasis were determined by intracellular staining (Fig. 5A–C; Supplementary Fig. S6). In spleen, percentages and total numbers of CD4<sup>+</sup> and CD8<sup>+</sup> T cells from D-CpG + OVA group had dramatically enhanced productions

of TNF $\alpha$ , IFN $\gamma$  and IL-2 (Fig. 5A–B). In TILs, CD4<sup>+</sup> T and CD8<sup>+</sup> T cells also produced significantly high TNF $\alpha$  and IFN $\gamma$  in D-CpG + OVA group (Fig. 5C). The percentages of IFN $\gamma$ -producing CD4<sup>+</sup> T and CD8<sup>+</sup> T cells and TNF $\alpha$ -producing CD8<sup>+</sup> T in TILs were also significantly higher in CpG + OVA group than PBS + OVA group. These data suggested that D-CpG + OVA promoted both tumor-specific CD4<sup>+</sup> and CD8<sup>+</sup> T-cell responses in terms of Th1 cytokine productions in lung



(caption on next page)

**Fig. 5. Antitumor response induced by the D-CpG included tumor vaccine in lung metastasis model was dependent on both CD4<sup>+</sup> and CD8<sup>+</sup> T cells.** Intracellular staining of TNF $\alpha$ , IFN $\gamma$  and IL2 by gating on CD4<sup>+</sup> (A) or CD8<sup>+</sup> (B) T cells from splenocytes stimulated with OVA protein. (C) Intracellular staining of TNF $\alpha$  and IFN $\gamma$  by gating on CD4<sup>+</sup> or CD8<sup>+</sup> T cells from TILs stimulated with OVA proteins. (D) Proliferations of CD4<sup>+</sup> and CD8<sup>+</sup> T cells were measured by <sup>3</sup>H-thymidine incorporation assay and PCNA expression using western blot. (E) Tetramer staining of OVA-specific CD8<sup>+</sup> T cells in TILs. (F) Cytotoxicity assay of splenocytes from the tumor-bearing mice. Splenocytes from tumor-bearing mice were incubated with OVA proteins for 5 days. Then, the splenocytes (effectors) were cocultured with B16-OVA (targets) at various E:T ratios using CytoTox 96 nonradioactive cytotoxicity assay. (G) Tumor foci of vaccine-treated mice with depletion of CD4<sup>+</sup> or/and CD8<sup>+</sup> T cells. In the depletion group, mice were injected i.p. with 1 mg GK1.5 (rat anti-mouse CD4 mAb) or/and 53-6.7 (rat anti-mouse CD8 mAb) 2 days before the first immunization. Mice were sacrificed on day 7 post the last immunization and the metastatic nodules were counted. The experiments were performed with 5–7 mice per group. The assays were done in quadruplicates. The data shown are the representative of three experiments. \**p* < 0.05 and \*\**p* < 0.01, \*\*\**p* < 0.001.

metastasis model.

The proliferations of both CD4<sup>+</sup> and CD8<sup>+</sup> T cells were enhanced after D-CpG + OVA immunization, as determined by <sup>3</sup>H-thymidine incorporation and PCNA expression (Fig. 5D). The percentages of OVA-specific CD8<sup>+</sup> T cells in TILs were significantly higher in D-CpG + OVA group (Fig. 5E). Splenocytes from mice immunized with D-CpG + OVA also exhibited a significantly high killing capacity against B16-OVA cells (Fig. 5F). All these results demonstrated that D-CpG + OVA promoted both tumor-specific CD4<sup>+</sup> and CD8<sup>+</sup> T-cell responses in lung metastasis model.

To determine whether CD4<sup>+</sup> and CD8<sup>+</sup> T cells were critical for antitumor activity induced by D-CpG + OVA, *in vivo* depletion of CD4<sup>+</sup> and/or CD8<sup>+</sup> T cells were performed in metastasis model (Fig. 5G). Depletion of CD8<sup>+</sup> T cells partially reduced the therapeutic effects of the vaccine, while depletion of CD4<sup>+</sup> has no effect on tumor growth. The therapeutic effects of D-CpG + OVA were totally inhibited by depletion of both CD4<sup>+</sup> and CD8<sup>+</sup> T cells. These results suggested that antitumor response induced by D-CpG + OVA was dependent on both CD4<sup>+</sup> and CD8<sup>+</sup> T cells.

To assess whether the anti-tumor response was limited against OVA, 1.5 × 10<sup>6</sup> T cells from D-CpG + OVA treated B16-OVA metastasis mice were isolated and adoptively transferred to mice *i.v.* injected with B16-F10 cells. No obviously therapeutic effects could be observed on B16-F10 tumor model after adoptive transfer of T cells from D-CpG + OVA immunized B16-OVA-bearing mice, suggested that anti-tumor response induced by D-CpG + OVA was limited against OVA (Fig. S7).

### 3.6. Decrease CD11b<sup>+</sup>Gr1<sup>low</sup> MDSCs subtype by D-CpG included tumor vaccine

In therapeutic models, D-CpG + OVA significantly decreased the percentages of CD11b<sup>+</sup>Gr1<sup>low</sup> subtype cells in spleen and tumor (Fig. 6A), while CpG + OVA dramatically enhanced the percentage of CD11b<sup>+</sup>Gr1<sup>low</sup> subtype cells in tumor. The percentages of CD11b<sup>+</sup>Gr1<sup>high</sup> subtype cells were not significantly different in each group. CD11b<sup>+</sup>Gr1<sup>low</sup> cells from tumor-bearing mice exhibited strongly inhibition of T cell proliferation, while CD11b<sup>+</sup>Gr1<sup>high</sup> cells exhibited a slight inhibition of T cell proliferation (Fig. 6C).

To define the therapeutic benefits by depletion of MDSCs, the anti-Gr1 antibodies were used to deplete MDSCs in vaccine-treated mice (Fig. 6D). Depletion of MDSCs significantly enhanced therapeutic effects in CpG group. Therapeutic effects of D-CpG + OVA were only slightly enhanced when combined with MDSCs depletion.

## 4. Discussion

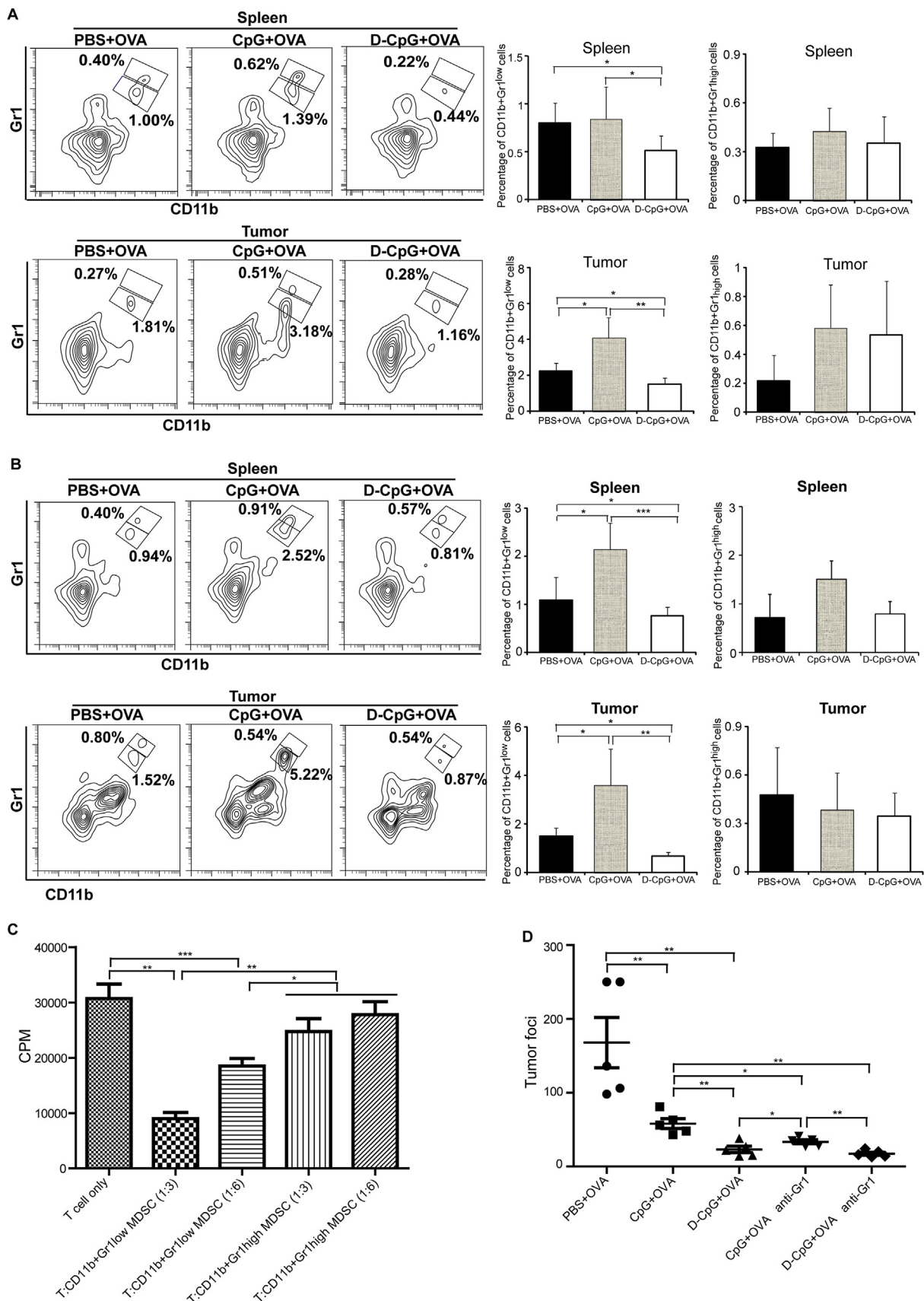
Stimulation of both tumor-specific Th1 and CTL responses has been one of the challenges for effective tumor vaccines. Adjuvants are often used to modulate the immune response types in vaccine development. We recently developed a new and lymph node targeting adjuvant by chemical conjugation type B CpG DNA with dextran polymer. To elucidate the possible antitumor mechanisms of this adjuvant, prophylaxis and therapeutic models of melanoma were used in this study. Our results demonstrated that this adjuvant can activate both tumor-specific Th1-polarized CD4<sup>+</sup> T cell and CTL responses and decreased the

percentage of CD11b<sup>+</sup>Gr1<sup>low</sup> cells in spleen and tumor.

Effector CD4<sup>+</sup> T can be divided into several subpopulations according to the cytokines they secreted. Th1, one of main antitumor mediators, is very important for the establishment and augmentation of tumor-specific CTL response, while Th2 and Treg cells inhibit antitumor immunity and promote the progression in patients with tumor [22–24]. The functional role of Th17 cells in tumor immunity remains still controversial [25]. Immunization of D-CpG + OVA dramatically increased both TNF $\alpha$  and IFN $\gamma$  productions in CD4<sup>+</sup> T cells. The antigen-specific IL4-or IL17-producing CD4<sup>+</sup> T cells were too few to be detected after D-CpG + OVA immunization. D-CpG-based vaccine enhanced Th1-mediate immune response in vaccination, instead of the Th2-like effects, which makes it an effective adjuvant for cancer immunotherapy. The higher percentages of Th1 and Tc1 in lung metastasis model than that of subcutaneous model suggested that D-CpG is inclined to stimulate Th1 and Tc1 responses in lung microenvironment.

CTL cells are considered to be the major player in cancer immunotherapy [26]. The increased proportion of TILs has been found to correlate with improved clinical outcome in several human cancers, such as ovarian cancer, melanoma, and prostate cancer [3,27]. Dextran-CpG conjugate markedly increased the uptake by antigen presenting cells in the lymph nodes, which is benefit for T cell activation [21]. Here, we found significantly high percentages of CD4<sup>+</sup> and CD8<sup>+</sup> T cells in tumor from D-CpG + OVA treated mice, compared with CpG + OVA or PBS + OVA treated mice. Many studies demonstrated that CpG could induce CTL response [28,29], which has been confirmed in our study with the high percentages of TNF $\alpha$ - and IFN $\gamma$ -producing CD8<sup>+</sup> T cells in TILs after CpG + OVA inoculation. Meanwhile, we also observed dramatic enhancement of TNF $\alpha$ - and IFN $\gamma$ -producing CD8<sup>+</sup> T cells in TILs and proliferation of antigen specific CD8<sup>+</sup> T cells after D-CpG + OVA inoculation, indicating an effective stimulation of CD8<sup>+</sup> T cells by D-CpG + OVA. Depletion experiments were carried out to determine the essential cells during antitumor immune response, and we found that antitumor immune response induced by D-CpG + OVA was dependent on both CD4<sup>+</sup> and CD8<sup>+</sup> T cells.

Adjuvants inclusion in vaccine formulations can stimulate and modulate the desirable immune responses to specific antigens. Protein without adjuvant always cannot stimulate any detectable immune responses (Fig. S7). Unlike in protective infectious diseases vaccines, cancer vaccines also need to overcome immunosuppressive effects of cells in tumor microenvironment. However, expected antitumor effects were obtained in only a limited number of clinical trials [30,31], as antitumor immunity is significantly suppressed by immunosuppressive cells presented in tumor microenvironment. MDSCs have crucial roles of immuno-suppression in tumor microenvironment [32–34]. MDSCs in mice can be identified by Gr-1<sup>+</sup>CD11b<sup>+</sup> phenotype, and can be further subdivided into granulocyte- or monocyte-like MDSCs according to their surface expression of the components of Gr1 antigen. CD11b<sup>+</sup>Gr1<sup>low</sup> cells resembling monocyte-like MDSCs are more immunosuppressive than CD11b<sup>+</sup>Gr1<sup>high</sup> cells resembling neutrophils or granulocyte-like MDSCs [35]. Present studies also demonstrated that only CD11b<sup>+</sup>Gr1<sup>low</sup> subtype cells could strongly suppress T cell proliferation. The prevalence, phenotypes and functions of MDSCs subtypes were associated with the immunization routes of CpG. For instance, systemic administration (e.g. subcutaneous injection) of CpG



(caption on next page)

**Fig. 6. Decrease CD11b<sup>+</sup>Gr1<sup>low</sup> MDSCs subtype by D-CpG included tumor vaccine.** (A) In subcutaneous melanoma model, vaccine-treated mice were sacrificed on day 18 after tumor inoculation. Percentages of MDSCs subtypes in spleen and tumor microenvironment were examined by staining of CD11b and Gr1. (B) In lung metastasis model, vaccine-treated mice were sacrificed on day 7 after the last vaccination. Percentages of MDSCs subtypes in spleen and tumor microenvironment were examined by staining of CD11b and Gr1. (C) Immunosuppressive functions of both MDSCs subtypes. CD8<sup>+</sup> T (50,000) cells from OT-1 mice were co-cultured with CD11b<sup>+</sup>Gr1<sup>low</sup> or CD11b<sup>+</sup>Gr1<sup>high</sup> cells isolated from tumor bearing mice at different ratios in the presence of 10,000 irradiated OVA-loaded DCs. <sup>3</sup>H-thymidine were added to the co-culture 72 h later. After another 16 h, the incorporation of <sup>3</sup>H-thymidine was measured with a liquid scintillation counter. (D) Therapeutic benefits by depletion of MDSCs. In the depletion group, mice were injected i.p. with 250 μg RB6-8C5 (rat anti-mouse Gr1 Ab) on the same day of vaccination, and the antibody injections were repeated 7 days later. Mice were sacrificed on day 7 post the last immunization and the metastatic nodules were counted. The experiments were performed with 5–7 mice per group. The assays were done in quadruplicates. The data shown are the representative of three experiments. \**p* < 0.05 and \*\**p* < 0.01, \*\*\**p* < 0.001.

increased the prevalence of MDSCs in the spleen and blood [36,37], while accumulation of CpG in tumor site from intratumor injection resulted in the reduction and inhibition of CD11b<sup>+</sup>Gr1<sup>low</sup> MDSC, as direct interaction of CpG and MDSCs inhibited CD11b<sup>+</sup>Gr1<sup>low</sup> MDSC [38]. Dextran is often employed as the LN and tumor targeting carrier [21], and conjugation with dextran leads to the accumulation of D-CpG in spleen and tumor after systemic injection, which may be the reason of the reduction of CD11b<sup>+</sup>Gr1<sup>low</sup> MDSC in spleen and tumor after s.c. injection of D-CpG. The status of immune checkpoint molecules was also examined. In tumor microenvironment, PD-1 expression on T cells was enhanced after CpG + OVA or D-CpG + OVA treatment. Previous study showed that IFN $\gamma$  promoted PD-L1 expression on tumor cells [39]. We also found that PD-L1 expression on tumor cells was also enhanced in D-CpG + OVA group, which may result from the increased expression of IFN $\gamma$  in this group. Therefore, combining with the Ab therapy targeting PD-L1 or PD-1 may further promote the therapeutic efficacy of D-CpG based tumor vaccine.

Thus, we demonstrated that D-CpG inclusion in vaccine formulations activated both tumor-specific Th1-polarized CD4<sup>+</sup> T cells and CTL responses *in vivo* and decreased the percentage of CD11b<sup>+</sup>Gr1<sup>low</sup> cells in the spleen and tumor.

#### Conflicts of interest

None.

#### Acknowledgements

This work has been supported by grants from the National Natural Science Foundation of China (grant numbers 31870918, 31500746), Natural Science Fund of Jiangsu Province (BK20170334, BK20171208), Open Project Program of Jiangsu Key Laboratory of Zoonosis (R1601), project funding from Suzhou City (grant numbers SNG2017047, SYS201677), and Project Funded by the Priority Academic Program Development of Jiangsu Higher Education Institutions.

#### Appendix A. Supplementary data

Supplementary data to this article can be found online at <https://doi.org/10.1016/j.canlet.2018.10.013>.

#### References

- H. Wang, H. Wei, R. Zhang, S. Hou, B. Li, W. Qian, et al., Genetically targeted T cells eradicate established breast cancer in syngeneic mice, *Clin. Canc. Res.* 15 (2009) 943–950.
- A. Schietinger, M. Philip, R.B. Liu, K. Schreiber, H. Schreiber, Bystander killing of cancer requires the cooperation of CD4(+) and CD8(+) T cells during the effector phase, *J. Exp. Med.* 207 (2010) 2469–2477.
- M.R.I. Young, Redirecting the focus of cancer immunotherapy to premalignant conditions, *Cancer Lett.* 391 (2017) 83–88.
- T. Scully, The age of vaccines, *Nature* 507 (2014) S2–S3.
- J.A. Berzofsky, J.D. Ahlers, I.M. Belyakov, Strategies for designing and optimizing new generation vaccines, *Nat. Rev. Immunol.* 1 (2001) 209–219.
- L. Villanueva, L. Silva, D. Llopiz, M. Ruiz, T. Iglesias, T. Lozano, et al., The Toll like receptor 4 ligand cold-inducible RNA-binding protein as vaccination platform against cancer, *Oncol Immunology* 7 (2017) e1409321.
- T. Kumai, S. Lee, H.I. Cho, H. Sultan, H. Kobayashi, Y. Harabuchi, et al., Optimization of peptide vaccines to induce robust antitumor CD4 T-cell responses, *Cancer Immunol. Res.* 5 (2017) 72–83.
- T. Kumai, S. Lee, H.I. Cho, H. Sultan, H. Kobayashi, Y. Harabuchi, et al., Optimization of peptide vaccines to induce robust antitumor CD4 T-cell responses, *Cancer Immunol. Res.* 5 (2017) 72–83.
- Y.L. Chen, M.C. Chang, Y.C. Chiang, H.W. Lin, N.Y. Sun, C.A. Chen, Immunomodulators enhance antigen-specific immunity and anti-tumor effects of mesothelin-specific chimeric DNA vaccine through promoting DC maturation, *Cancer Lett.* 425 (2018) 152–163.
- J.S. Rudra, B.N. Banasik, G.N. Milligan, A combined Carrier-adjunct system of peptide nanofibers and toll-like receptor agonists potentiates robust CD8+ T cell responses, *Vaccine* 36 (2018) 438–441.
- A. Arias, M. Vicario, D. Bernardo, J.M. Olalla, M. Fortea, A. Montalban-Arques, et al., Toll-like receptors-mediated pathways activate inflammatory responses in the esophageal mucosa of adult eosinophilic esophagitis, *Clin. Transl. Gastroenterol.* 9 (2018) 147.
- U. Ohto, H. Ishida, T. Shibata, R. Sato, K. Miyake, T. Shimizu, Toll-like receptor 9 contains two DNA binding sites that function cooperatively to promote receptor dimerization and activation, *Immunity* 48 (2018) 649–658.
- M. Veleeparambil, D. Poddar, S. Abdulkhalek, P.M. Kessler, M. Yamashita, S. Chattopadhyay, et al., Constitutively bound EGFR-mediated tyrosine phosphorylation of TLR9 is required for its ability to signal, *J. Immunol.* 200 (2018) 2809–2818.
- E.M. Doorduyn, M. Sluiter, D.C. Salvatori, S. Silvestri, S. Maas, R. Arens, et al., CD4<sup>+</sup> T Cell and NK cell interplay key to regression of MHC Class I<sup>low</sup> tumors upon TLR7/8 agonist therapy, *Cancer Immunol. Res.* 5 (2017) 642–653.
- J. Wu, D.J. Waxman, Immunogenic chemotherapy: dose and schedule dependence and combination with immunotherapy, *Cancer Lett.* 419 (2018) 210–221.
- E. Müller, P.F. Christopoulos, S. Halder, A. Lunde, K. Beraki, M. Speth, et al., Toll-like receptor ligands and interferon- $\gamma$  synergize for induction of antitumor M1 macrophages, *Front. Immunol.* 8 (2017) 1383.
- M. Ebrahimian, M. Hashemi, M. Maleki, K. Abnous, G. Hashemitarbar, al et al., Induction of a balanced Th1/Th2 immune responses by co-delivery of PLGA/ovalbumin nanospheres and CpG ODNs/PEI-SWCNT nanoparticles as TLR9 agonist in BALB/c mice, *Int. J. Pharm.* 515 (2016) 708–720.
- S. Wang, J. Campos, M. Gallotta, M. Gong, C. Crain, E. Naik, et al., Intratumoral injection of a CpG oligonucleotide reverts resistance to PD-1 blockade by expanding multifunctional CD8+ T cells, *Proc. Natl. Acad. Sci. U. S. A.* 113 (2016) E7240–E7249.
- J. Li, J. Ge, S. Ren, T. Zhou, Y. Sun, H. Sun, et al., Hepatitis B surface antigen (HBsAg) and core antigen (HBcAg) combine CpG oligodeoxynucleotides as a novel therapeutic vaccine for chronic hepatitis B infection, *Vaccine* 33 (2015) 4247–4254.
- X. Li, L. Guo, M. Kong, X. Su, D. Yang, M. Zou, et al., Design and evaluation of a multi-epitope peptide of human Metapneumovirus, *Intervirology* 58 (2015) 403–412.
- W. Zhang, M. An, J. Xi, H. Liu, Targeting CpG adjuvant to lymph node via dextran conjugate enhances antitumor immunotherapy, *Bioconjug. Chem.* 28 (2017) 1993–2000.
- M.J. Dobrzanski, Expanding roles for CD4 T cells and their subpopulations in tumor immunity and therapy, *Front. Oncol.* 3 (2013) 63.
- S.E. Church, S.M. Jensen, P.A. Antony, N.P. Restifo, B.A. Fox, Tumor-specific CD4<sup>+</sup> T cells maintain effector and memory tumor-specific CD8<sup>+</sup> T cells, *Eur. J. Immunol.* 44 (2014) 69–79.
- E.M. Janssen, N.M. Droin, E.E. Lemmens, M.J. Pinkoski, S.J. Bensinger, B.D. Ehst, et al., CD4<sup>+</sup> T-cell help controls CD8<sup>+</sup> T-cell memory via TRAIL-mediated activation-induced cell death, *Nature* 434 (2005) 88–93.
- Y. Mei, L. Zhao, Y. Liu, H. Gong, Y. Song, L. Lei, et al., Combining DNA vaccine and AIDA-1 in attenuated *Salmonella* activates tumor-specific CD4<sup>+</sup> and CD8<sup>+</sup> T-cell responses, *Cancer Immunol. Res.* 5 (2017) 503–514.
- F.S. Basingab, M. Ahmadi, D.J. Morgan, IFN $\gamma$ -dependent interactions between ICAM-1 and LFA-1 counteract prostaglandin E2-mediated inhibition of antitumor CTL responses, *Cancer Immunol. Res.* 4 (2016) 400–411.
- M. Harao, M.A. Forget, J. Roszik, H. Gao, G.V. Babiera, S. Krishnamurthy, et al., 4-1BB-enhanced expansion of CD8<sup>+</sup> TIL from triple-negative breast cancer unveils mutation-specific CD8<sup>+</sup> T cells, *Cancer Immunol. Res.* 5 (2017) 439–445.
- H. Tian, Y. He, X. Song, L. Jiang, J. Luo, Y. Xu, et al., Nitrate T helper cell epitopes enhance the immunogenicity of HER2 vaccine and induce anti-tumor immunity, *Cancer Lett.* 430 (2018) 79–87.
- K. Kobiyama, B. Temizoz, T. Kanuma, K. Ozasa, M. Momota, T. Yamamoto, et al., Species-dependent role of type I IFNs and IL-12 in the CTL response induced by humanized CpG-complexed with  $\beta$ -glucan, *Eur. J. Immunol.* 46 (2016) 1142–1151.
- H.T. Kissick, M.G. Sanda, The role of active vaccination in cancer immunotherapy:

- lessons from clinical trials, *Curr. Opin. Immunol.* 35 (2015) 15–22.
- [31] C. Ghirelli, T. Hagemann, Targeting immunosuppression for cancer therapy, *J. Clin. Invest.* 123 (2013) 2355–2357.
- [32] A. Li, H.B. Barsoumian, J.E. Schoenhals, T.R. Cushman, M.S. Caetano, X. Wang, et al., Indoleamine 2,3-dioxygenase 1 inhibition targets anti-PD1-resistant lung tumors by blocking myeloid-derived suppressor cells, *Cancer Lett.* 431 (2018) 54–63.
- [33] P. Serafini, Myeloid derived suppressor cells in physiological and pathological conditions: the good, the bad, and the ugly, *Immunol. Res.* 57 (2013) 172–184.
- [34] H. Zhang, Z.L. Li, S.B. Ye, L.Y. Ouyang, Y.S. Chen, J. He, et al., Myeloid-derived suppressor cells inhibit T cell proliferation in human extranodal NK/T cell lymphoma: a novel prognostic indicator, *Cancer Immunol. Immunother.* 64 (2015) 1587–1599.
- [35] X. Zhan, Y. Fang, S. Hu, Y. Wu, K. Yang, C. Liao, et al. IFN- $\gamma$  differentially regulates subsets of Gr-1(+)/CD11b(+) myeloid cells in chronic inflammation. *Mol. Immunol.* 66:451-462.
- [36] S. Morecki, Y. Gelfand, E. Yacovlev, O. Eizik, Y. Shabat, S. Slavin, CpG-induced myeloid CD11b<sup>+</sup>Gr-1<sup>+</sup> cells efficiently suppress T cell-mediated immunoreactivity and graft-versus-host disease in a murine model of allogeneic cell therapy, *Biol. Blood Marrow Transplant.* 14 (2008) 973–984.
- [37] M.F. Harman, R.P. Ranocchia, C.V. Gorlino, M.F. Sánchez Vallecillo, S.D. Castell, M.I. Crespo, et al., Expansion of myeloid-derived suppressor cells with arginase activity lasts longer in aged than in young mice after CpG-ODN plus IFA treatment, *Oncotarget* 6 (2015) 13448–13461.
- [38] Y. Shirota, H. Shirota, D.M. Klinman, Intratumoral injection of CpG oligonucleotides induces the differentiation and reduces the immunosuppressive activity of myeloid-derived suppressor cells, *J. Immunol.* 188 (2012) 1592–1599.
- [39] J. Chen, Y. Feng, L. Lu, H. Wang, L. Dai, Y. Li, et al., Interferon- $\gamma$ -induced PD-L1 surface expression on human oral squamous carcinoma via PKD2 signal pathway, *Immunobiology* 217 (2012) 385–393.